



Published in final edited form as:

*Circ Res.* 2007 April 13; 100(7): e72–e80. doi:10.1161/01.RES.0000264101.06417.33.

## Autonomic Nerve Stimulation reverses Ventricular Repolarization Sequence in Rabbit Hearts

Rajkumar Mantravadi<sup>1,4</sup>, Bethann Gabris<sup>4</sup>, Tong Liu<sup>4</sup>, Bum-Rak Choi<sup>2,4</sup>, William C. de Groat<sup>3</sup>, G. André Ng<sup>1</sup>, and Guy Salama<sup>4,5</sup>

<sup>1</sup> Department of Cardiovascular Sciences, Cardiology group, University of Leicester, UK

<sup>2</sup> Department of Biomedical Engineering, Tulane University, New Orleans, LA 70118

<sup>3</sup> Department of Pharmacology, University of Pittsburgh, Pittsburgh, PA 15261

<sup>4</sup> Department of Cell biology and Physiology, University of Pittsburgh, Pittsburgh, PA 15261

### Abstract

Sympathetic activity and spatial dispersion of repolarization (DOR) have been implicated as mechanisms that promote arrhythmia vulnerability yet there are no direct measurements of the effects of autonomic nerve stimulation on DOR. Rabbit hearts were perfused in a Langendorff apparatus with full sympathetic and parasympathetic innervation, and were optically mapped to measure action potential durations (APDs) and DOR (Apex-Base) over the left ventricles. DOR was measured under sinus rhythm, during bilateral sympathetic nerve stimulation (SNS) and right and/or left vagus nerve stimulation (VNS) and was compared to DOR during isoproterenol (100 nM) or acetylcholine (1  $\mu$ M) infusion. In sinus rhythm, repolarization started at the apex and systematically progressed towards the base. SNS (10–15 Hz) increased DOR by 29% (from  $\Delta$ APD =  $17 \pm 0.7$  to  $-22 \pm 1.6$  ms, n=6) and reversed DOR as the direction of repolarization from apex  $\rightarrow$  base in sinus rhythm shifted to base  $\rightarrow$  apex in 5–15 s after SNS. DOR flipped-back to its sinus rhythm DOR pattern  $115 \pm 15$  s after the interruption of SNS. During right or left VNS, there was no change in the direction of DOR but bilateral VNS increased and reversed DOR to base  $\rightarrow$  apex direction. Infusion of isoproterenol or acetylcholine increased DOR but did not alter the direction of repolarization sequences. These findings demonstrate that bilateral autonomic activity (SNS or VNS) cause reversible shifts of apex-base DOR and that the spatial heterogeneities of autonomic effects on the ventricles are most likely due to a greater innervation at the base than the apex of the heart.

### Keywords

Autonomic Nerve Stimulation; Sympathetic Nerve Stimulation; Vagus Nerve Stimulation; Dispersion of Repolarization; Action Potential Durations and Optical Mapping

### Introduction

Cardiac repolarization is the cumulative manifestation of ion channel kinetics, spatial distributions of channel expression, cell-cell coupling and their modulation by autonomic nerve activity and circulating hormones. At the cellular level, repolarization is determined

<sup>5</sup>To whom all correspondence should be addressed: Guy Salama Ph.D., Professor of Cell Biology and Physiology, University of Pittsburgh, School of Medicine, 3500 Terrace Street, S312 Biomedical Science Tower, Pittsburgh, PA 15261, Phone: (412) 648-9354; Fax: (412) 648-8330 gsalama@pitt.edu.

by the current amplitudes, activation and inactivation kinetics of ion channels; that in most mammalian hearts include: voltage-gated  $\text{Na}^+$  ( $I_{\text{Na}}$ ) and L-Type  $\text{Ca}^{2+}$  ( $I_{\text{Ca,L}}$ ) channels, the fast and slow components of delayed rectifier  $\text{K}^+$  channels ( $I_{\text{Kr}}$  and  $I_{\text{Ks}}$ ), and the fast component of the transient  $\text{K}^+$  channel ( $I_{\text{to,f}}$ ).<sup>1-4</sup> At the organ level, the dispersion of repolarization (DOR) is a measure of the non-uniformity of repolarization, most likely caused by regional differences in ion channel distribution from endocardium to epicardium<sup>5-7</sup> and along the epicardium from apex to base of the ventricles.<sup>8-11</sup>

In hearts under sinus rhythm, repolarization sequences have been obtained from the surface of mouse,<sup>12, 13</sup> guinea pig<sup>14-17</sup> and rabbit<sup>18, 19</sup> hearts using optical mapping techniques. In all animal models tested thus far, repolarization was shown to proceed from the apex to the base of the heart and to be independent of the activation sequence and to depend on intrinsic differences of APDs.<sup>20</sup> Transmural DOR was measured from isolated canine wedge preparations and found to differ significantly when paced on the endocardium (to mimic sinus rhythm) compared to epicardium.<sup>21</sup>

*In vivo*, adrenergic regulation of the heart occurs by two dominant mechanisms: a) direct delivery of catecholamine through sympathetic nerve activity and b) humoral secretion of catecholamine in the circulation by the adrenal glands. Humoral actions of catecholamine on cardiac electrophysiology can be investigated by infusing adrenergic agonists in the perfusion solution in animal studies or injections in the blood stream of volunteers.<sup>22, 23</sup> In contrast, studies on the effects of autonomic nerve activity on APD are sparse.<sup>24</sup> and there are no reports on the neuromodulation of DOR.

Enhanced DOR and dynamic properties of APDs such as the steepness of the APD restitution kinetics curve and APD (or T wave) alternans have been shown to promote arrhythmias.<sup>25-27</sup> Adrenergic agonists and/or autonomic imbalance may enhance DOR and promote T wave alternans and/or steeper APD restitution curve by modulating ionic currents and their kinetics in a spatially heterogeneous manner and therefore alter repolarization dynamics.<sup>28</sup> Transmural dispersions of repolarization have been implicated as a contributing factor to arrhythmia vulnerability in canine and human studies.<sup>5</sup> There is also substantial evidence in support of enhanced DOR over the surface of the ventricles as a mechanism to increase the vulnerability to re-entrant arrhythmia, in animal models and human hearts.<sup>13, 26, 29</sup> Although there are no direct measurements of DOR and T wave alternans during autonomic nerve activity, numerous studies have emphasized the importance of behavioral states and emotional stress (i.e. high autonomic activity) as triggers of T wave alternans, and risk for sudden cardiac death.<sup>30, 31</sup>

In this report, we modified the isolated, innervated rabbit heart preparation reported by Ng et al.,<sup>24</sup> by setting up two perfusion circuits one for the autonomic nerves, the other to perfuse the heart in a modified Langendorff apparatus that allowed us to maintain physiological pressure and flow rates to the heart. The arrangement improved the staining of the heart with a voltage sensitive dye and the delivery of drugs while retaining functional sympathetic and parasympathetic innervation for several hours. APDs and DOR were measured during bilateral sympathetic nerve stimulation (SNS) or during right or left or bilateral vagus nerve stimulation (VNS). Changes in bipolar electrograms, optical maps of APDs were measured continuously for up to 10 minutes, before, during and after SNS or VNS. The combination of optical mapping and intact, fully innervated heart preparation provides a unique tool to investigate important topics in neurocardiology.

## Methods

### Heart preparations

Fully innervated rabbit hearts were isolated using a modified method of that described by Ng et al.,<sup>24</sup> Briefly, adult New Zealand white rabbits (3.5–4 kg,  $n = 14$ ) were pre-medicated with Ketamine HCl (0.1 mg kg<sup>-1</sup>, s.c. Hospira Inc USA) and Medetomidine (1mg s.c, Pfizer) followed by general anesthesia induced and maintained by Diprivan (Astra Zeneca 1–2 mg kg<sup>-1</sup>, i.v.). Rabbits were ventilated, after tracheotomy, using a small-animal ventilator (Harvard Apparatus Ltd, Edenbridge, Kent, UK, 60 breaths per min) with an O<sub>2</sub>/air mixture. The vagus nerves were isolated and the blood vessels leading to and from the ribcage were ligated and dissected. The rabbit was euthanized with sodium pentobarbital and portions of the rib cage were removed and the descending aorta was cannulated. The pericardium was cut and ice-cold Tyrode's solution was applied to the surface of the heart to preserve myocardial function. The preparation extending from the neck to thorax was dissected from surrounding tissues as described previously.<sup>24</sup> All procedures were undertaken in accordance with the Animals (Scientific Procedures) Act 1986 and the current *Guide for the Care and Use of Laboratory Animals* Published by the US National Institutes of Health (NIH Publication No. 85–23, revised 1985).

A new method was devised to improve dye and drug delivery to the heart and improve cardiac perfusion pressure and coronary flow rate. Two perfusion circuits were set up with two peristaltic pumps. One pump perfused the spinal cord from the descending aorta to the spinal artery, at low flow rates (10–15 ml/min). The other perfused the heart in a modified Langendorff apparatus at a higher constant flow rate (30 ml/min) by inserting a 5 French catheter (B. Braun Medical Inc., Bethlehem, PA) up the ascending aorta above the aortic valve and inflating the balloon catheter to maintain perfusion pressure to the heart (65±5 mmHg) and to separate the two perfusion circuits. This approach was critical to stain the heart with the voltage sensitive dye, obtain reproducible drug actions at reasonable concentrations and achieve physiological perfusion pressures to the heart and the spinal cord. The heart and nerves were perfused with Tyrode's solution containing (in mM): 130 NaCl, 24 NaHCO<sub>3</sub>, 1.0 CaCl<sub>2</sub>, 1.0 MgCl<sub>2</sub>, 4.0 KCl, 1.2 NaH<sub>2</sub>PO<sub>4</sub>, 20 dextrose, at pH 7.4, and gassed with 95% O<sub>2</sub> plus 5% CO<sub>2</sub> at 37 °C ± 1 °C. Hearts were stained with the voltage sensitive dye, di-4 ANEPPS (40 µl of a 1 mg/ml stock solution in dimethyl sulfoxide). Two methods were used in combination to reduce motion artifacts: 1) The heart was placed horizontally in a custom designed chamber with an adjustable base and 2 straps to hold a glass slide against the region of epicardium to mechanically immobilize the region viewed by the photodiode array (Fig. 1). 2) Cytochalasin-D was used sparingly at 2µM in the perfusate for 10 min followed by washout. When applied in this manner, Cytochalasin-D reduced contractions for 20–30 min without altering AP characteristics, conduction velocity or repolarization.

### Optical apparatus

The optical apparatus was previously described.<sup>18</sup> Briefly, light from two 100-W tungsten-halogen lamps was collimated and passed through 520 ± 30 nm interference filters. Fluorescence emitted from the stained heart was collected with a camera lens. Fluorescence emission from the anterior region of heart was passed through a cutoff filter (610 nm, Omega Optical, Brattleboro, VT, USA) and focused on a 16 × 16 elements photodiode array (C4675-103, Hamamatsu Corp., Bridgewater, NJ, USA) (Fig. 1). Outputs from the photodiode array were amplified, digitized (14-bit) at 1,000 frames/s (Microstar Laboratories, Inc., Bellevue, WA, USA) and were acquired for at least 40 s for subsequent data analysis.

## Nerve Stimulation and Image Acquisition protocols

**Sympathetic Nerve Stimulation**—A quadripolar electrode was inserted in the spinal canal at the 12th thoracic vertebra and the tip was advanced to the level of the 2nd thoracic vertebra to stimulate cardiac sympathetic outflow. From previous reports, SNS and VNS tolerated stimulation frequencies of up to 20 Hz and 15 V, without noticeable run down of the autonomic responses, measured as changes in heart rate and developed pressure.<sup>24</sup> In this study SNS were kept at a sub-maximum stimulation strength of 15 Hz and 15 V for 50 s or until the maximum change of heart rate occurred<sup>24</sup> then the stimulus was turned off to allow heart rate to return to baseline. Vagus nerves were stimulated individually (right or left) or simultaneously with silver chloride bipolar electrodes (15 V, 15Hz for 5 s) producing a drop in the heart rate to < 100 beats/min. A stimulus generator was custom-made in the electronic shop of University of Pittsburgh to control the stimuli from 1–20 V and 1–20 Hz.

**Data Analysis:** APDs were measured from the optical APs recorded at each site from the difference between the activation and repolarization time points, as previously described.<sup>15</sup> The activation time point was calculated from the maximum first derivative of the AP upstroke,  $(dF/dt)_{\max}$  which represented the time when most of the cells viewed by a diode fired an AP and the repolarization time point was calculated from the maximum second derivative of the AP downstroke,  $(d^2F/dt^2)_{\max}$ .<sup>15</sup> We previously showed that the inflection point,  $(d^2F/dt^2)_{\max}$  represents the refractory period of the AP based on extra stimuli applied at 1.5X threshold voltage. The second derivative fell at 97% and 90–96% recovery to baseline for APs recorded respectively, with a microelectrode or optically.<sup>15</sup> In hearts with a prominent plateau phase, such as the rabbit (but not the mouse or rat AP), the maximum second derivative of the AP downstroke provided a unique time point that is not distorted by motion artifacts. In addition, the second derivative algorithm offered a major advantage in that it was impervious to low levels of motion artifacts compared to APD70 or APD90.<sup>15</sup> All parameters, APDs, DOR, AI (Activation intervals) and HR (heart rate) were expressed as the mean  $\pm$  SEM. Comparisons were made using student T-test on paired samples.<sup>14, 29, 32</sup> Comparisons were made between paired samples and T-test was used to test the significance. P value of <0.05 was considered statistically significant. The isochronal lines (2 ms interval) were drawn using custom written software using IDL (Interactive Data Language).

## Results

### Effects of Autonomic Nerve Stimulation and Perfusion with neurotransmitters on heart rate

Figure 2 illustrates the time course of heart rate changes elicited by SNS (A), bilateral VNS (B), or perfusion with isoproterenol (C) or acetylcholine (D). All four interventions were applied until the maximum change in heart rate was reached then the intervention was stopped. As shown in panels A and B, the interruption of autonomic nerve stimulation resulted in the recovery of the heart rate back to its original value in seconds. In contrast, the wash out of neurotransmitters and the reversal of their effects on heart rate was considerably slower requiring several minutes (Note time scale in Figure 2, panels: C and D). Bipolar electrogram recordings were made continuously to verify that the hearts remained in sinus rhythm throughout the measurements. Electrogram recordings are illustrated for each intervention, before (traces a), during (traces b) and after (traces c) the application of SNS (A), VNS (B), ISO (C) and ACH (D). In all the hearts analyzed, activation under sinus rhythm lasted  $6 \pm 2$  ms ( $n = 30$ ) and the patterns did not vary significantly (not shown).

## Sympathetic Nerve Stimulation

Stimulation of the spinal canal to induce SNS increased heart rate gradually from  $143 \pm 6.3$  (AI =  $427 \pm 18.3$  ms) to a peak rate of  $229 \pm 13.2$  beats/min (AI =  $265 \pm 13.2$  ms) (Figure 2A). More remarkable, SNS changed the direction of repolarization from apex towards the base (control: CTRL) to base towards the apex (Table 1,  $n = 7$ ). Figure 3A illustrates a map of repolarization gradient and a series of 16 superimposed APs from apex to base at slow and fast sweep speeds, during sinus rhythm (CTRL) prior to SNS. Figure 3B shows the same measurement from the same heart after 50 s of SNS at 15 Hz. The reversal of the direction of repolarization during SNS was due to difference of its effects at the base and apex of the ventricles. As shown in Table 1, SNS did not significantly change APDs at the apex (Control: APD =  $159 \pm 4.2$ , during SNS APD =  $155 \pm 12$  ms;  $p = \text{NS}$ ) whereas SNS caused a marked shortening of APDs at the Base ( $134 \pm 9.3$  ms) compared to sinus rhythm (APD =  $176 \pm 4.0$  ms;  $p < 0.001$ ;  $n=7$ ). DOR during sinus rhythm (APD base-APD apex) was  $17 \pm 0.7$  ms and during SNS, DOR changed to  $-22 \pm 1.6$  ms; ( $p < 0.001$ ), ( $n = 7$ ); meaning that the direction of repolarization was reversed due to heterogeneities of the effects SNS being more pronounced at the base than at the apex.

## Sinus Rhythm vs. Isoproterenol Infusion

Isoproterenol infusion (100 nM) increased heart rate to  $204 \pm 13.1$  beats/min ( $n = 6$ ) ( $p = 0.0289$ ) and DOR to  $23 \pm 1.6$  ms ( $p < 0.01$ ,  $n = 5$ ) (Figure 2C) but did not change the direction of repolarization, which remained from apex to base. Figure 4A and B compares maps of APDs recorded from the same heart first in sinus rhythm (CTRL) and 2 min after perfusion with 100 nM isoproterenol (ISO).

## Time course of DOR changes Caused by SNS

Upon SNS, DOR reversed from apex  $\rightarrow$  base to base  $\rightarrow$  apex by 15 s and when SNS stimulation was stopped, heart rate returned to baseline and DOR returned to control values and to its original orientation (i.e. apex to base) with a latency of  $115 \pm 15$  s. Figure 5 depicts the changes in DOR as a function of time for 4 hearts where DOR was mapped before, during 50 s of SNS and 150 s after the interruption of SNS. The slower recovery of DOR of  $\sim 2$  min implicates a cellular signaling process but the possibility of a slow redistribution of neurotransmitter (i.e. norepinephrine) or a slow dissociation constant from its receptor cannot be excluded.

## Vagus Nerve Stimulation (VNS)

Right vagus nerve stimulation (VNS), caused a gradual drop in heart rate to  $95 \pm 4.5$  beats/min ( $n=6$ ) and DOR did not change significantly in magnitude or direction (Table 1). Left VNS caused a significant a similar drop in heart rate as for right VNS ( $96 \pm 5.8$  beats/min), failed to produce a statistically significant change DOR and did not reverse the orientation of repolarization (Table 1). In contrast, bilateral VNS reversed the direction of repolarization from apex  $\rightarrow$  base to base  $\rightarrow$  apex with  $\Delta\text{APD} = -16 \pm 2$  ms during bilateral VNS. Figure 3A, C, D and E compares maps of repolarization from the same during sinus rhythm (A: CTRL), right VNS (C: VNSR), left VNS (D: VNSL) and bilateral VNS (E: VNSBL). Bilateral VNS reversed the repolarization sequence due to its different effects at the base and apex of the ventricles. APDs at the apex increased significantly during bilateral VNS compared to sinus rhythm, from  $159 \pm 4.2$  to  $195 \pm 14$  ms ( $n = 6$ ;  $p < 0.02$ ) which may be attributed in large part to the decrease in heart rate from  $143 \pm 6.3$  to  $91 \pm 6.6$  beats/min (Table 1). At the base, however, bilateral VNS did not cause a statistically significant APD prolongation from  $176 \pm 4.0$  ms in sinus rhythm to  $178 \pm 13.8$  ms with bilateral VNS (Table 1). When compared to the anticipated APD prolongation observed by pacing at long cycle

lengths, bilateral VNS failed to produce the APD prolongation expected from the slower heart rate.

### Sinus Rhythm vs. Acetylcholine infusion

Perfusion with acetylcholine (1  $\mu$ M) to mimic parasympathetic nerve activity decreased heart rate to  $105 \pm 10.2$  beats/min with significant increase in (DOR  $32 \pm 3.0$  ms) but without any change in the direction of repolarization sequence (Table 1). Figure 4C illustrates a repolarization map and the superposition of APs (apex  $\rightarrow$  base) that were recorded during perfusion with Ach (1  $\mu$ M). As shown in Figure 4C, repolarization advanced from apex to base, similar to repolarization sequence recorded in the absence of autonomic nerve activity.

### Effects of Autonomic Nerve Stimulation on the Repolarization Sequence

Figure 6 summarizes the changes in DOR measured on the left ventricle of rabbit hearts during SNS, right, left and bilateral VNS compared to isoproterenol or acetylcholine perfusion. The averaged data reveals a statistically significant reversal of the repolarization sequence, being oriented from apex  $\rightarrow$  base in controls to base  $\rightarrow$  apex during SNS or bilateral VNS. Changes in the magnitude of DOR can be attributed to rate and cellular signaling effects caused by norepinephrine and acetylcholine but the reversals of the repolarization sequence implicate spatial heterogeneities of autonomic nerves along the apex-base axis.

## Discussion

The main findings are that autonomic (bilateral either sympathetic or parasympathetic) nerve stimulation changes DOR on the epicardium in a manner distinct from perfusion with a  $\beta$ -adrenergic or cholinergic agonist (see Figure 6). In particular, autonomic nerve stimulation was found to bring about a reversal of the direction of repolarization along the apex to base axis of the heart. The reversal of DOR had a rapid onset of  $< 15$  s after SNS and upon stopping SNS, DOR reversed back to sinus rhythm DOR, with a latency of  $\sim 2$  min. Perfusion with isoproterenol produced similar increases in heart rate as those obtained by SNS, yet there was no reversal of DOR. Similarly, bilateral VNS produced the expected decrease in heart rate and reversed the direction of repolarization whereas perfusion with Ach produced a similar decrease in heart rate but did not reverse DOR.

It is important to emphasize that the stimulation of the autonomic nerves described in this study followed previous protocols that were shown to be physiological with respect to a) changes in heart rate and b) left ventricular developed pressure.<sup>24</sup> Changes in the latter parameters during SNS were entirely blocked by a selective  $\beta_1$  adrenergic antagonist, Metoprolol (1.8  $\mu$ M) and during VNS by a muscarinic antagonist, Atropine (0.1  $\mu$ M) indicating that autonomic nerve stimulation modulated the heart by the standard neurotransmitters.<sup>24</sup> In the current experiments, autonomic nerve stimulation produced changes in heart rate in the physiological range that were highly reproducible from heart-to-heart and were reversible upon interruption of nerve stimulation. In addition, we were able to obtain multiple repetitions (3–4) of SNS and VNS on the same heart without significant run down of the autonomic nerves based on the cardiac responses.

### Ventricular Repolarization

Ventricular activation sequences have been extensively characterized in intact hearts by mapping the time delays of QRS spikes measured from closely spaced extracellular bipolar electrodes.<sup>33</sup> In contrast, the repolarization sequence or recovery to baseline has been poorly defined in large part due to technical difficulties and the sensitivity of that process to



numerous variables. Changes in heart rate, temperature depth of anesthesia, sympathetic tone and electrolyte balance all influence the action potential duration locally and thus, ventricular repolarization. Action potentials can be recorded from the epicardial surface with microelectrodes or suction electrodes but only from a limited number of sites, leaving surface electrograms as the most practical method to track activation and repolarization sequences.<sup>33</sup> However, unlike activation, there is no electrogram deflection that accurately identifies the onset or termination of repolarization. Nevertheless, local activation recovery intervals (ARI) measured with surface electrodes (i.e. activation time point (minimum dV/dt of the QRS complex) minus the recovery (maximum dV/dt of the T-wave) time-point) were used as a surrogate for APDs measured with an intracellular electrode. In early studies on dog hearts, ventricular repolarization determined from ARI produced opposite findings; with repolarization sequence proceeding from base to apex<sup>34</sup> or apex to base.<sup>35</sup> Although there was a good correlation between ARI and refractory periods and APDs, most ARI were shorter than refractory periods<sup>36</sup> and differed from APDs by as much as 24 ms.<sup>37</sup> Alternatively, repolarization sequences determined from the local refractory periods indicated that repolarization and APD gradients proceeds from base to apex (short to-long APDs) *in situ* dog hearts.<sup>38, 39</sup> A more recent study on canine and human hearts reported the opposite result that APDs are shorter in ventricular myocytes from the apex than the base due to higher densities of K<sup>+</sup> currents involved in ventricular repolarization.<sup>11</sup>

The advent of voltage sensitive dyes and optical mapping techniques has provided new tools to characterize ventricular repolarization.<sup>40</sup> In isolated perfused hearts, ventricular repolarization was found to proceed from apex to base in a wide range of species: a) mouse,<sup>12, 41</sup> b) rat,<sup>42</sup> c) guinea pig,<sup>14</sup> d) rabbit,<sup>32</sup> and e) perhaps dog and human hearts. In all these species, repolarization is driven by a different set of ion channels yet their spatial distribution preserve short to long APDs in going from apex to base so as to guide the sequence of repolarization and relaxation.

### Anatomical Distribution of Autonomic Nerves to the Heart

Sympathetic outflow to the heart emerges from the thoracic intermedio-lateral horns of the spinal cord. Pre-ganglionic neurons in the spinal cord project to the heart via axonost postganglionic neurons to innervate the heart via paravertebral ganglia and the various thoracic and cardiac ganglia.<sup>43, 44</sup> Studies on dogs reported that different branches of the sympathetic nerves innervated distinct regions of the ventricles but there is a controversy regarding such specific anatomical nerve distribution. In our experiment, spinal canal stimulation at the level of T2 vertebrae allowed us to broadly activate bilaterally the sympathetic nerves thus, circumventing potential controversies, inaccuracies and animal-to-animal variability of cardiac nerve distribution.<sup>45, 46</sup>

### Effects and Mechanism of Sympathetic Activity on DOR

Changes in APD during SNS were heterogeneous and striking. During the SNS, DOR not only increased across the ventricle but its direction was inverted. Under control conditions, APDs were longer at the base than the apex whereas during SNS, APDs at the base were significantly shorter than at the apex. Changes of DOR upon SNS occurred rapidly in 5–15 s and DOR reversed back to control orientation but with a slower time-course of 1300 to 140 s. These findings are consistent with current concepts in the literature that the autonomic nerves and delayed rectifying K<sup>+</sup> channels involved in the repolarization of the heart are heterogeneously distributed along the apex to base axis of the heart. In human hearts, autonomic nerves (both sympathetic and parasympathetic) are considerably more abundant at the base than the apex of left ventricles.<sup>47</sup> The delayed rectifying K<sup>+</sup> currents are non-uniform on the surface of the heart, with the slow component, I<sub>Ks</sub> being more abundant at the base and the fast component I<sub>Kr</sub> being more abundant at the apex of the rabbit left

ventricle.<sup>32, 48</sup> Moreover,  $I_{Ks}$  tends to be a weak current, difficult to measure until activated by a  $\beta$ -adrenergic agonist such as isoproterenol which decreases the refractory period by a protein kinase A-dependent phosphorylation of  $I_{Ks}$  but has no effect on  $I_{Kr}$ .<sup>49, 50</sup> Therefore in the absence of sympathetic activity,  $I_{Kr}$  dominates and repolarization advances from apex to base. In contrast, during SNS, activation of  $I_{Ks}$  by norepinephrine is more abundant at the base resulting in greater APD shortening at the base than at the apex and a reversal of the repolarization sequence. The preferential shortening of APDs at the base under sympathetic influence occurred in  $\sim 15$  s (i.e. time to phosphorylate  $I_{Ks}$ ) and was reversible upon interruption of SNS with a latency of 180 s consistent with the time-course of  $I_{Ks}$  dephosphorylation.<sup>49</sup>

Interestingly, perfusion of the heart with isoproterenol had a tendency to enhance DOR (Table 1) by shortening APDs slightly more at the apex than the base but the direction of repolarization was not reversed. These data highlight the complexity of the system because SNS releases norepinephrine, a  $\beta$ - and  $\alpha$ -adrenergic agonist that stimulates nearly all ionic currents and their kinetics. In addition, SNS may activate afferent as well efferent nerves and release other neurotransmitters such as neuropeptide Y, ATP and substance P. Nevertheless, the results from the isoproterenol perfusion allows us to reasonably conclude that regional (apex-base) heterogeneities of sympathetic innervation (efferent and/or afferent nerves) is the dominant factor responsible for the reversal of DOR during SNS rather than  $I_{Kr}$ ,  $I_{Ks}$  or  $\beta_1$  adrenergic receptor distribution across the ventricle.<sup>28</sup>

### Effects and Mechanism of Parasympathetic Activity on DOR

Right or left VNS did not change the DOR significantly but bilateral VNS reversed the direction of DOR, this time by prolonging APD more at the apex than the base. All 3 methods of VNS decreased heart rate to the same extent so that differences in APD caused by the 3 conditions cannot be attributed to heart rate alone (Table 1 and Figure 5) but to enhanced recruitment of parasympathetic and acetylcholine release during bilateral VNS. Acetylcholine released by vagus nerves may shorten ventricular APDs by increasing the  $K^+$  conductance via the muscarinic receptors in the ventricle.<sup>51</sup> Immuno-histochemistry<sup>47</sup> of parasympathetic nerve distribution to the ventricle suggests a greater density of nerves at the base than the apex which may explain the lack of APD prolongation at the base despite the slow heart rate during bilateral VNS. Thus, as for SNS, the effects of VNS on DOR are most likely due to heterogeneities in nerve distribution resulting in the modulation of the repolarization sequence.

Neuronal modulation of ventricular repolarization is unique and distinct from pharmacological modulation. These findings reveal that under physiological conditions autonomic activity has a marked impact on cardiac repolarization and broaden our views on why and how 'autonomic imbalance' may be an important factor contributing to arrhythmia vulnerability during physical or emotional stress. Further studies are needed to elucidate the effects of autonomic nerve activity on transmural repolarization, on hearts with long QT or ischemia to gain deeper insights into the contribution of neural activity to arrhythmia vulnerability.

### Acknowledgments

The study was supported by awards from the National Institutes of Health, RO1 HL57929 and HL70722 to G. Salama



## References

1. Curran ME, Splawski I, Timothy KW, et al. A molecular basis for cardiac arrhythmia: HERG mutations cause long QT syndrome. *Cell* Mar 10;1995 80(5):795–803. [PubMed: 7889573]
2. Wang Q, Shen J, Splawski I, et al. SCN5A mutations associated with an inherited cardiac arrhythmia, long QT syndrome. *Cell* Mar 10;1995 80(5):805–811. [PubMed: 7889574]
3. Wang Q, Curran ME, Splawski I, et al. Positional cloning of a novel potassium channel gene: KVLQT1 mutations cause cardiac arrhythmias. *Nat Genet* Jan;1996 12(1):17–23. [PubMed: 8528244]
4. Splawski I, Timothy KW, Decher N, et al. Severe arrhythmia disorder caused by cardiac L-type calcium channel mutations. *Proc Natl Acad Sci U S A* Jun 7;2005 102(23):8089–8096. discussion 8086–8088. [PubMed: 15863612]
5. Antzelevitch C. Role of transmural dispersion of repolarization in the genesis of drug-induced torsades de pointes. *Heart Rhythm* Nov;2005 2(2 Suppl):S9–15. [PubMed: 16253930]
6. Antzelevitch C, Belardinelli L. The role of sodium channel current in modulating transmural dispersion of repolarization and arrhythmogenesis. *J Cardiovasc Electrophysiol* May;2006 17( Suppl 1):S79–S85. [PubMed: 16686686]
7. Antzelevitch C. Transmural dispersion of repolarization and the T wave. *Cardiovasc Res* Jun;2001 50(3):426–431. [PubMed: 11376617]
8. Brahmajothi MV, Morales MJ, Rasmusson RL, et al. Heterogeneity in K<sup>+</sup> channel transcript expression detected in isolated ferret cardiac myocytes. *Pacing Clin Electrophysiol* Feb;1997 20(2 Pt 2):388–396. [PubMed: 9058843]
9. Nerbonne JM, Guo W. Heterogeneous expression of voltage-gated potassium channels in the heart: roles in normal excitation and arrhythmias. *J Cardiovasc Electrophysiol* Apr;2002 13(4):406–409. [PubMed: 12033361]
10. Szabo G, Szentandrassy N, Biro T, et al. Asymmetrical distribution of ion channels in canine and human left-ventricular wall: epicardium versus midmyocardium. *Pflugers Arch* Aug;2005 450(5): 307–316. [PubMed: 15952036]
11. Szentadrassy N, Banyasz T, Biro T, et al. Apico-basal inhomogeneity in distribution of ion channels in canine and human ventricular myocardium. *Cardiovasc Res* Mar 1;2005 65(4):851–860. [PubMed: 15721865]
12. Baker LC, London B, Choi BR, et al. Enhanced dispersion of repolarization and refractoriness in transgenic mouse hearts promotes reentrant ventricular tachycardia. *Circ Res* Mar 3;2000 86(4): 396–407. [PubMed: 10700444]
13. London B, Baker LC, Petkova-Kirova P, et al. Dispersion of Repolarization and Refractoriness are Determinants of Arrhythmia Phenotype in Transgenic Mice with long QT. *J Physiol*. Nov 16;2006
14. Salama G, Lombardi R, Elson J. Maps of optical action potentials and NADH fluorescence in intact working hearts. *Am J Physiol* Feb;1987 252(2 Pt 2):H384–94. [PubMed: 3812752]
15. Efimov IR, Huang DT, Rendt JM, et al. Optical mapping of repolarization and refractoriness from intact hearts. *Circulation* Sep;1994 90(3):1469–1480. [PubMed: 8087954]
16. Efimov IR, Ermentrout B, Huang DT, et al. Activation and repolarization patterns are governed by different structural characteristics of ventricular myocardium: experimental study with voltage-sensitive dyes and numerical simulations. *J Cardiovasc Electrophysiol* Jun;1996 7(6):512–530. [PubMed: 8743757]
17. Rosenbaum DS, Kaplan DT, Kanai A, et al. Repolarization inhomogeneities in ventricular myocardium change dynamically with abrupt cycle length shortening. *Circulation* Sep;1991 84(3): 1333–1345. [PubMed: 1884456]
18. Choi BR, Salama G. Simultaneous maps of optical action potentials and calcium transients in guinea-pig hearts: mechanisms underlying concordant alternans. *J Physiol* Nov 15;2000 529(Pt 1): 171–188. [PubMed: 11080260]
19. Liu T, Choi BR, Drici MD, et al. Sex modulates the arrhythmogenic substrate in prepubertal rabbit hearts with Long QT 2. *J Cardiovasc Electrophysiol* May;2005 16(5):516–524. [PubMed: 15877623]

20. Kanai A, Salama G. Optical mapping reveals that repolarization spreads anisotropically and is guided by fiber orientation in guinea pig hearts. *Circ Res* Oct;1995 77(4):784–802. [PubMed: 7554126]
21. Fish JM, Di Diego JM, Nesterenko V, et al. Epicardial activation of left ventricular wall prolongs QT interval and transmural dispersion of repolarization: implications for biventricular pacing. *Circulation* May 4;2004 109(17):2136–2142. [PubMed: 15078801]
22. Magnano AR, Holleran S, Ramakrishnan R, et al. Autonomic modulation of the u wave during sympathomimetic stimulation and vagal inhibition in normal individuals. *Pacing Clin Electrophysiol* Nov;2004 27(11):1484–1492. [PubMed: 15546302]
23. Magnano AR, Talathoti N, Hallur R, et al. Sympathomimetic infusion and cardiac repolarization: the normative effects of epinephrine and isoproterenol in healthy subjects. *J Cardiovasc Electrophysiol* Sep;2006 17(9):983–989. [PubMed: 16879629]
24. Ng GA, Brack KE, Coote JH. Effects of direct sympathetic and vagus nerve stimulation on the physiology of the whole heart—a novel model of isolated Langendorff perfused rabbit heart with intact dual autonomic innervation. *Exp Physiol* May;2001 86(3):319–329. [PubMed: 11471534]
25. Riccio ML, Koller ML, Gilmour RF Jr. Electrical restitution and spatiotemporal organization during ventricular fibrillation. *Circ Res* Apr 30;1999 84(8):955–963. [PubMed: 10222343]
26. Pak HN, Hong SJ, Hwang GS, et al. Spatial dispersion of action potential duration restitution kinetics is associated with induction of ventricular tachycardia/fibrillation in humans. *J Cardiovasc Electrophysiol* Dec;2004 15(12):1357–1363. [PubMed: 15610278]
27. Nearing BD, Verrier RL. Modified moving average analysis of T-wave alternans to predict ventricular fibrillation with high accuracy. *J Appl Physiol* Feb;2002 92(2):541–549. [PubMed: 11796662]
28. Conrath CE, Opthof T. Ventricular repolarization: An overview of pathophysiology, sympathetic effects and genetic aspects. *Prog Biophys Mol Biol*. Jul 12;2005
29. Choi BR, Liu T, Salama G. The distribution of refractory periods influences the dynamics of ventricular fibrillation. *Circ Res* Mar 16;2001 88(5):E49–58. [PubMed: 11249880]
30. Verrier RL, Antzelevitch C. Autonomic aspects of arrhythmogenesis: the enduring and the new. *Curr Opin Cardiol* Jan;2004 19(1):2–11. [PubMed: 14688627]
31. Verrier RL, Dickerson LW, Nearing BD. Behavioral states and sudden cardiac death. *Pacing Clin Electrophysiol* Sep;1992 15(9):1387–1393. [PubMed: 1384002]
32. Choi BR, Burton F, Salama G. Cytosolic Ca<sup>2+</sup> triggers early afterdepolarizations and Torsade de Pointes in rabbit hearts with type 2 long QT syndrome. *J Physiol* Sep 1;2002 543(Pt 2):615–631. [PubMed: 12205194]
33. Burgess MJ, Baruffi S, Spaggiari S, et al. Determination of activation and recovery sequences and local repolarization durations from distant electrocardiographic leads. *Jpn Heart J* Nov;1986 27( Suppl 1):205–216. [PubMed: 3820586]
34. Massumi RA, Pipberger H, Prinzmetal M, et al. Studies on the nature of the repolarization process. XIX. Studies on the mechanism of ventricular activity. *Am Heart J* Jan;1957 53(1):100–124. [PubMed: 13381701]
35. Haas HG. Contribution to the theory of the ventricular gradient. *Cardiologia* 1960;36:321–336. [PubMed: 13710194]
36. Millar CK, Kralios FA, Lux RL. Correlation between refractory periods and activation-recovery intervals from electrograms: effects of rate and adrenergic interventions. *Circulation* Dec;1985 72(6):1372–1379. [PubMed: 4064279]
37. Haws CW, Lux RL. Correlation between in vivo transmembrane action potential durations and activation-recovery intervals from electrograms. Effects of interventions that alter repolarization time. *Circulation* Jan;1990 81(1):281–288. [PubMed: 2297832]
38. Burgess MJ, Green LS, Millar K, et al. The sequence of normal ventricular recovery. *Am Heart J* Nov;1972 84(5):660–669. [PubMed: 4639740]
39. Autenrieth G, Surawicz B, Kuo CS. Sequence of repolarization on the ventricular surface in the dog. *Am Heart J* Apr;1975 89(4):463–469. [PubMed: 1114977]
40. Salama G, Choi BR. Images of Action Potential Propagation in Heart. *News Physiol Sci* Feb;2000 15:33–41. [PubMed: 11390873]

41. London B, Baker LC, Petkova-Kirova P, et al. Dispersion of repolarization and refractoriness are determinants of arrhythmia phenotype in transgenic mice with long QT. *J Physiol* Jan 1;2007 578(Pt 1):115–129. [PubMed: 17110412]
42. Wan B, Doumen C, Duszynski J, et al. Effects of cardiac work on electrical potential gradient across mitochondrial membrane in perfused rat hearts. *Am J Physiol* Aug;1993 265(2 Pt 2):H453–460. [PubMed: 8368348]
43. VI, S. *Physiology of Autonomic Ganglia*. Tokyo: Igaku Shoin; 1973.
44. Armour JA. Cardiac neuronal hierarchy in health and disease. *Am J Physiol Regul Integr Comp Physiol* Aug;2004 287(2):R262–271. [PubMed: 15271675]
45. Opthof T, Misier AR, Coronel R, et al. Dispersion of refractoriness in canine ventricular myocardium. Effects of sympathetic stimulation. *Circ Res* May;1991 68(5):1204–1215. [PubMed: 2018987]
46. Gillespie JS, Muir TC. A method of stimulating the complete sympathetic outflow from the spinal cord to blood vessels in the pithed rat. *Br J Pharmacol Chemother* May;1967 30(1):78–87. [PubMed: 4382677]
47. Kawano H, Okada R, Yano K. Histological study on the distribution of autonomic nerves in the human heart. *Heart Vessels* Mar;2003 18(1):32–39. [PubMed: 12644879]
48. Cheng J, Kamiya K, Liu W, et al. Heterogeneous distribution of the two components of delayed rectifier K<sup>+</sup> current: a potential mechanism of the proarrhythmic effects of methanesulfonanilideclass III agents. *Cardiovasc Res* Jul;1999 43(1):135–147. [PubMed: 10536698]
49. Sanguinetti MC, Jurkiewicz NK, Scott A, et al. Isoproterenol antagonizes prolongation of refractory period by the class III antiarrhythmic agent E-4031 in guinea pig myocytes. Mechanism of action. *Circ Res* Jan;1991 68(1):77–84. [PubMed: 1984874]
50. Volders PG, Stengl M, van Opstal JM, et al. Probing the contribution of IKs to canine ventricular repolarization: key role for beta-adrenergic receptor stimulation. *Circulation* Jun 3;2003 107(21):2753–2760. [PubMed: 12756150]
51. Koumi S, Sato R, Nagasawa K, et al. Activation of inwardly rectifying potassium channels by muscarinic receptor-linked G protein in isolated human ventricular myocytes. *J Membr Biol* May 1;1997 157(1):71–81. [PubMed: 9141360]

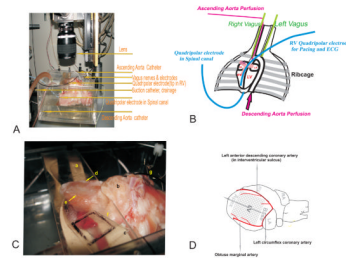


**Figure 1. Isolated innervated heart Preparation**

**A:** Side view of the heart-nerve preparation. The photograph shows the heart immobilized between a glass slide above and rubber slings (brown) below. This keeps the heart in position for optical mapping.

**B:** Schematic of the isolated innervated heart preparation. The heart was placed in a custom-made chamber for optical mapping of APs. PA: Pulmonary artery; LV: Left Ventricle, RV: Right ventricle; The Ascending Aorta was perfused with a 5f pulmonary wedge monitoring balloon catheter inserted in the right carotid artery. A quadripolar electrode was placed in the right ventricle via the pulmonary artery and used to pace the heart or measure a bipolar electrogram. A second quadripolar electrode was inserted in the spinal canal and used to stimulate the thoracic out-flow of the sympathetic trunk at T2 level.

**C** A close-up view of the heart in position for optical mapping. Small letters describe the following structures: a) Elastic rubber slings were placed posterior to the heart to immobilize the anterior surface against a glass slide. b) Thymus gland and associated fat pads. c) Glass slide with a transparent marker for exact positioning of the preparation. Note that the dark border has the dimensions of the optical field-of-view. d) Left anterior descending artery in the interventricular *sulcus*. e) Obtuse marginal artery. f) Left atrium. g) Right vagus nerve placed on stimulating electrodes.

**D.** Schematic of the mapped region. The supine position of the heart held by rubber straps stabilizes an area of the left ventricle between the interventricular *sulcus* and the obtuse marginal artery that was mapped optically (area shown as a grid).

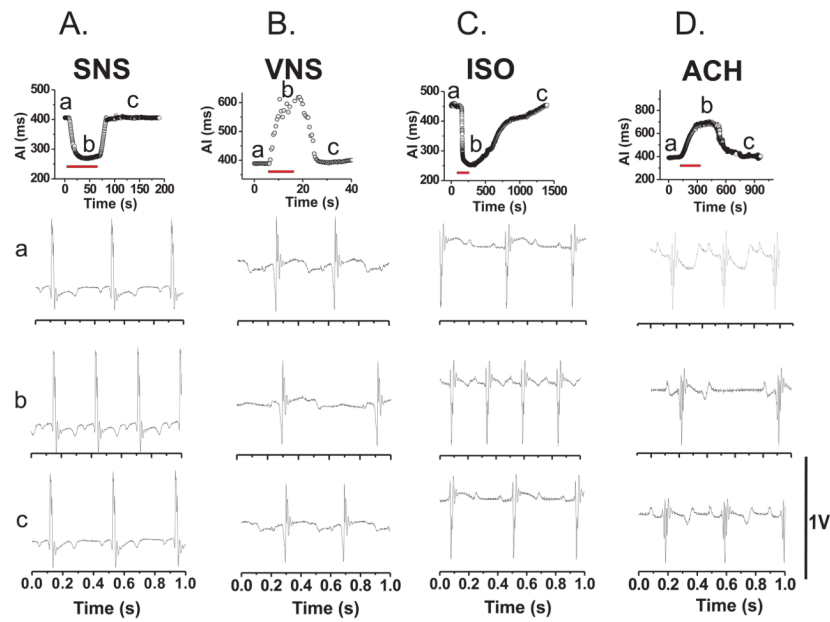


**Figure 2. Changes in Activation Intervals (AI) and electrogram recordings as a function of time** Changes in AI were plotted as a function of time during sinus rhythm before (a), during (b) and (c) after a physiological intervention. Below each plot, Electrogram recordings are shown for three phases of these experiments (a) before, (b) during, and (c) after recovery from an intervention. The duration of each intervention is shown as a red line. AI: Activation interval (milliseconds); A.SNS: Sympathetic nerve stimulation; B.VNS: bilateral vagus nerve stimulation; C.ISO: isoproterenol (100 nM) infusion; D.ACH: infusion of Acetylcholine (1  $\mu$ M).

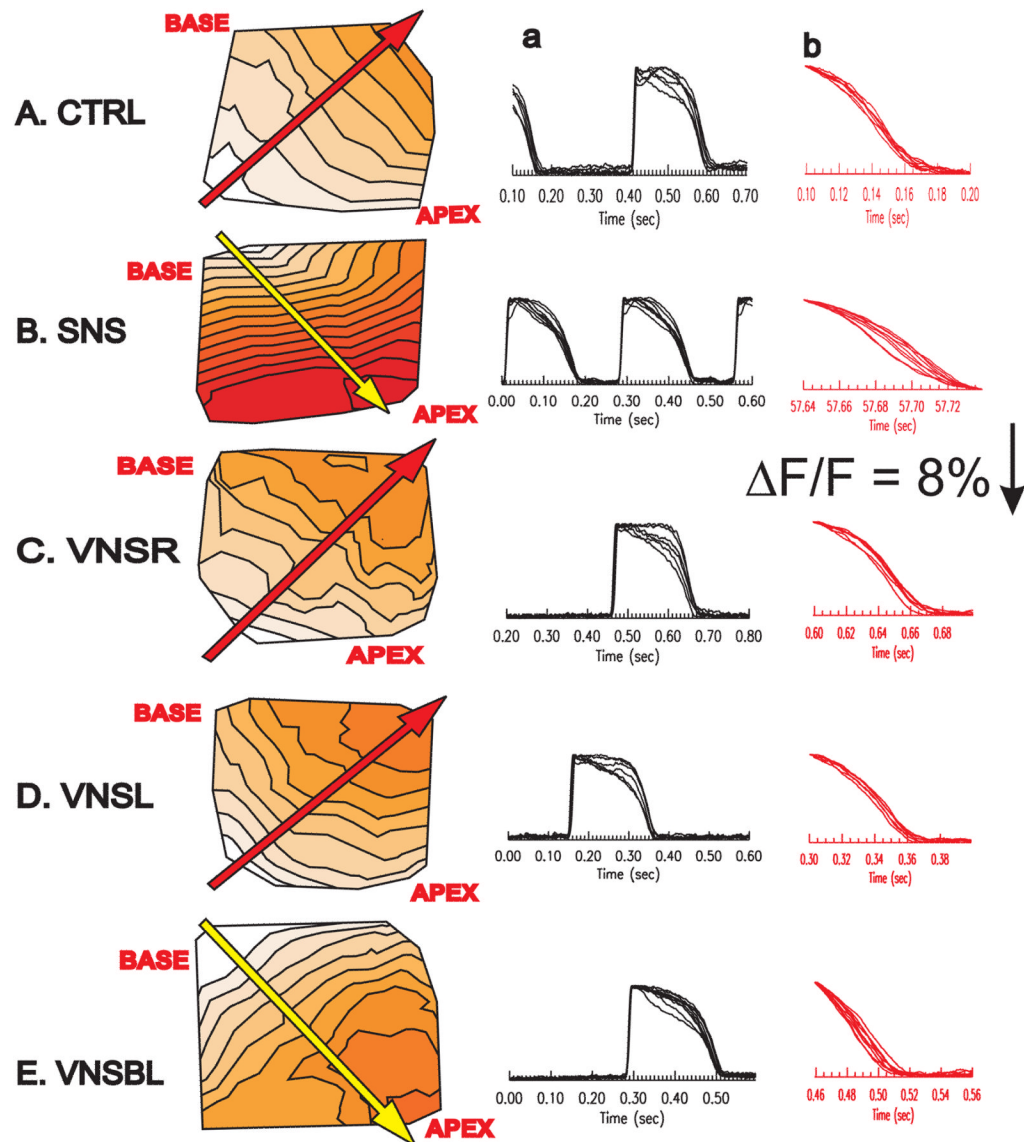


**Figure 3. Effects of Sympathetic Neuromodulation of Apex-Base DOR**

CTRL: control; SNS: Sympathetic nerve stimulation; VNSR: Right vagus stimulation; VNSL: left vagus stimulation; VNSBL: bilateral vagus nerve stimulation. The dispersion of repolarization is mapped with isochronal lines (time difference between successive isochronal lines is 2 ms). Light to dark shades represent early to late repolarization time-points. Arrow points to the direction of repolarization sequence. Traces (a) illustrate the superposition of APs (aligned in time) from different locations on the heart and differences of APDs across the surface. Traces (b) display the same traces at a faster sweep speed to visualize temporal differences in AP downstroke.



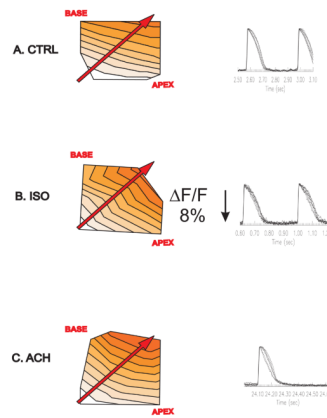


**Figure 4. Pharmacological modulation of (apex-base) DOR**

CTRL: control; ISO: Isoproterenol; ACH: Acetylcholine infusion. DOR is mapped with isochronal lines (2 ms apart). Light to dark shades represent early to late repolarization time-points. Arrow points to the direction of repolarization. Note there is no change in the direction of the repolarization sequence caused by the adrenergic or muscarinic agonists. Isochronal lines are 2 ms apart.

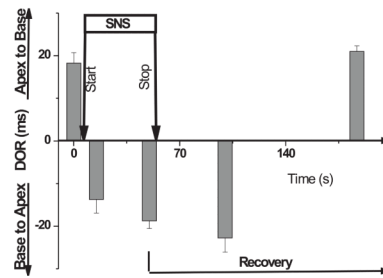


**Figure 5. Dynamic changes of DOR during SNS and recovery**

Time-course of changes in DOR before, during and after sympathetic nerve stimulation (n=4 hearts). DOR was inverted within 15 s after SNS and remained inverted in some experiments for as long as 15 min (not shown) whereas recovery had a longer latency of  $115 \pm 15$  s after the interruption of SNS. After the interruption of SNS at peak heart rate ( $\sim 50$  s), different hearts reversed their DOR at different times. More precisely, the earliest reversal occurred at 115 s in 1 out of 4 hearts, 3 hearts reversed at  $165 \pm 5$  s and one heart at 180 s.

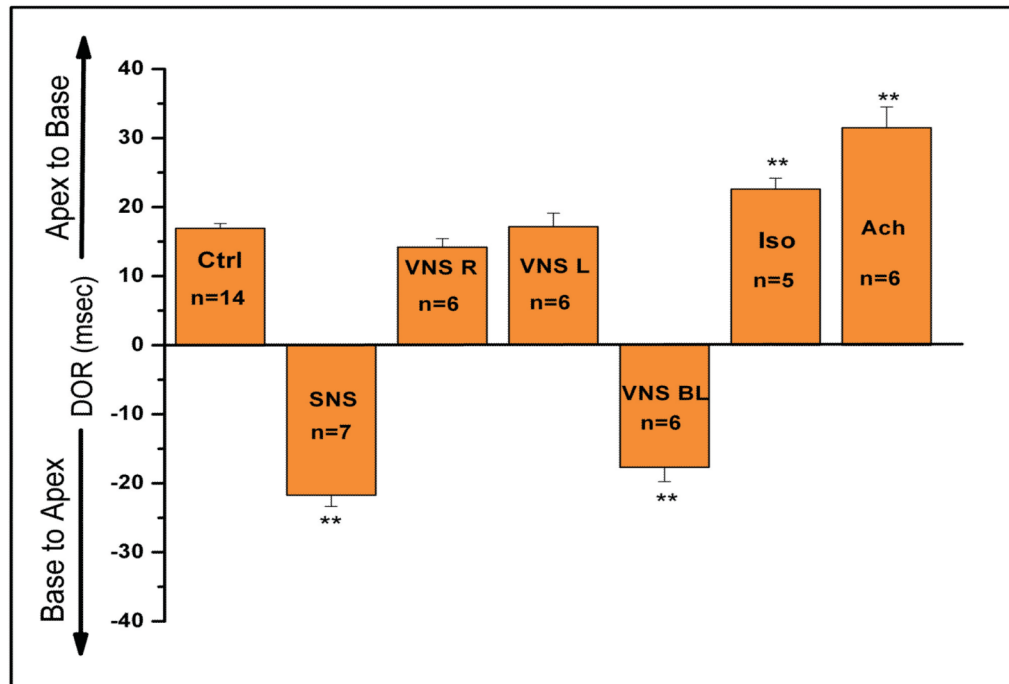


**Figure 6. Summary of autonomic modulation of DOR**

(A): Summary of DOR changes in sinus rhythm compared to various autonomic nerve stimulation protocols. n= the number of rabbit hearts tested. CTRL: control; SNS: Sympathetic nerve stimulation; VNSR: Right vagus stimulation; VNSL: left vagus stimulation; VNSBL: bilateral vagus nerve stimulation; Iso: Isoproterenol (100 nM); Ach: Acetylcholine (1 $\mu$ M); \*\*P < 0.05 Paired t-test vs. control

**Table 1**

Changes in Heart Rate, APDs and DOR during SNS and VNS

	HR (beats/min)	APD Apex (ms)	APD Base (ms)	DOR (ms)
Control n = 14	143 ± 6.3	159 ± 4.2	176 ± 4.0	17 ± 0.7
SNS n = 7	229 ± 13.2*	155 ± 12.0	134 ± 9.3*	-22 ± 1.6*
ISO n = 5	204 ± 13.1*	115 ± 4.4*	138 ± 5.0*	23 ± 1.6*
L VNS n = 6	96 ± 5.8*	165 ± 13.5	182 ± 11.9	17 ± 2.0
R VNS n = 6	95 ± 4.5*	170 ± 10.5	185 ± 9.5	13 ± 1.8
BL VNS n = 6	91 ± 6.6*	195 ± 14*	178 ± 13.8	-16 ± 2.0*
Ach n = 6	105 ± 10.2*	178 ± 19.0	204 ± 18.3	32 ± 3.0*

Changes in heart rate, APD at the apex and the base and their difference or DOR were measured during autonomic stimulation. L, R and BL VNS: Left, Right and Bilateral Vagus Nerve Stimulation; Ach: Acetylcholine infusion (1  $\mu$ M); Isoproterenol (100 nM), APD: Action potential duration; DOR: dispersion of repolarization (measured as the difference in APD (Base-Apex); n: number of rabbit hearts,

\*  $p < 0.05$  by paired t-test was considered statistically significant compared to sinus rhythm values. Note the regional alterations in APDs during nerve stimulation did not occur during perfusion with isoproterenol or Ach.